

The Impact of Slope Roughness on the Uncertainty in Probabilistic Rockfall Modelling

Indishe Senanayake¹, Philipp Hartmann¹, Klaus Thoeni¹, Abigail Watman¹, Anna Giacomini¹

¹Centre for Geotechnical Science and Engineering, The University of Newcastle, Callaghan, NSW 2308, Australia.

E-mail: indishe.senanayake@newcastle.edu.au

Abstract: Rockfall simulations play a crucial role in assessing rockfall hazards and designing mitigation measures. A very common approach in industry is to perform probabilistic rockfall simulations on the basis of idealized 2D profiles. Highwalls in open cuts are generally considered as a single slope segment with artificially introduced roughness. This study assesses the uncertainty associated with such single slope profile rockfall simulations with respect to the energy at first impact at the base of the wall as well as runout distance. The results of single slope rockfall simulations are compared against simulations performed using sophisticated 2D sections extracted from four different photogrammetric derived 3D high-resolution rock wall models. In the results, it is shown that the energy at first impact is similar for both simplified and natural slopes but with higher variability of energy for natural slopes. In contrast, the runout distances are always underestimated by the simplified slopes compared to natural slopes. These disparities are associated with the inability of simplified single-line-segment slopes to accurately represent the irregularity in natural slopes. Hence, the results indicate the importance of rockfall simulations performed with slopes extracted from high-resolution 3D models for more realistic results.

Keywords: Probabilistic modelling; Rockfalls; Runout distance; Surface roughness; Lumped mass model.

1 Introduction

Rockfalls are major hazards in mountainous terrains, in open pit mines with sub-vertical rock exposures and rock-cuts for roads and railways. Rockfalls are commonly triggered by structural, climatic or mechanical initiations, which lead to single rock blocks or debris of rock material to detach and fall with a rapid downward motion. The rockfall trajectory is generally characterized by falling, bouncing, rolling and sliding phases. These falling blocks pose a great threat to lives and infrastructure (Deparis et al., 2011; Wyllie, 2015). Therefore, identifying rockfall hazards, predicting rockfall trajectories and analyzing the uncertainty of existing simulation approaches play a crucial role in minimizing the associated risks (Wyllie, 2015).

The prediction of a rockfall trajectory, in particular of the rockfall runout and energy at the bottom of a slope, is a fundamental step for the design of the most appropriate mitigation measure and its location. Over the past few decades, different approaches have been considered and implemented to minimize the rockfall hazard including empirical, geographic information system (GIS) based and process-based methods (Dorren, 2003). Among these methods, process-based approaches are, generally, developed using probabilistic modelling and by simulating the physics of a rock falling along a slope. Probabilistic approaches, in particular, can account for the uncertainties associated with rockfall scenarios, and provide more reliable results which are closer to realistic variability of in-situ rockfall conditions (Pfeiffer and Bowen, 1989).

Probabilistic rockfall simulations using idealized two-dimensional (2D) profiles are a very common approach in industry, especially at mine planning and development phases. Here, highwalls in open cuts are often considered as a single slope segment with artificially introduced roughness and normal, k_n , and tangential coefficient of restitution, k_t , values assigned to the slope and floor materials. Lumped mass models are often employed in these approaches where the mass of falling blocks is considered as a single dimensionless point. Ferrari et al. (2016) conducted a 2D stochastic sensitivity analysis on rockfall runout distance and energy of the first impact at the base of a rockface. A 2D slope geometry simplified by an inclined single-line-segment was considered in the simulations. 78,400 rockfall scenarios with a large range of input parameters and their combinations were considered. Slope angle α , vertical height h , standard deviation σ_r for roughness, k_n and k_t were used as input variables in these simulations. The results evidence that the energy at first impact and runout distance are mainly driven by σ_r and α , whereas k_n and k_t play a secondary role. However, in the application of such an approach significant uncertainties remain associated with the idealized representation of the 2D slope profile by a single-line-segment as natural rock slopes often consist of high irregularity of roughness and slope angles.

The current study intends to assess and compare the contribution of the slope roughness to runout distance and energies at first impact by using 2D slope profiles extracted from (i) single-line-segments with synthetically introduced roughness parameters and (ii) natural 3D rockfaces. For the latter, 2D sections are extracted from photogrammetric derived high-resolution 3D rock wall models and rockfall scenarios are simulated with respect to the natural roughness (i.e., without synthetically introduced roughness values). For the former, a series of single-line-

segment 2D sections is created using combinations of α and σ_r values within the same range of 2D sections extracted from the natural rockfaces. Here, the σ_r values are synthetically introduced by using RocFall (Rocscience). The runout distance and energy at first impact at the base of the wall are calculated with respect to rockfalls initiated at different heights by simulating rockfall scenarios with single-line-segment slopes. The runout distances and energies are compared against the results of natural rockfaces with similar α and σ_r values at each height. The obtained results provide new insights into the risks associated with the uncertainty of 2D rockfall simulations conducted with single-line-segment profiles.

2 Methodology

2.1 Overview

This study evaluates the uncertainties associated with rockfall simulations performed using single-line-segment 2D slope profiles with synthetically introduced roughness parameters. The simulation results of single-line-segment slopes are compared against the results of 2D slices extracted from the 3D rock walls with natural roughness. These 3D meshes have been generated by triangulating photogrammetric derived high-resolution pointclouds of open-cut mine walls. Based on the distribution of local slope angles of individual 2D slices the associated standard deviation σ_r for the roughness is calculated. The α and σ_r ranges considered for the single-line-segment profiles are chosen in alignment with the extracted ranges of the 2D natural slope profiles. In the following, the photogrammetric derived 3D rock walls are denoted ‘3D walls’, the 20 m segments of these walls ‘wall segments’, and the 2D sections extracted from these segments as ‘2D slices’ (Figure 1). Note that the extracted 2D slices consist of local slope segments between vertices.

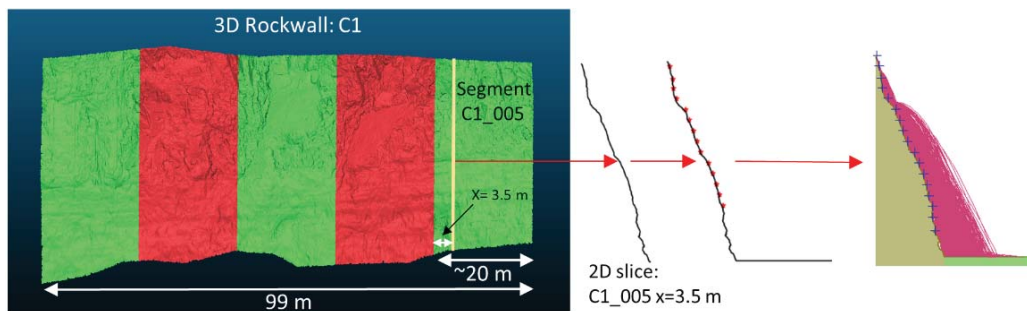


Figure 1. An example representation of photogrammetric derived 3D rockwall (C1), 20 m segments, a 2D slice extracted at $x = 3.5$ m from the segment, the manipulated slice by adding a floor and initial block release positions (red points) and RocFall simulation.

The simulations are performed using RocFall 8.017 (Rocscience, 2021) with blocks thrown at different heights for both slope categories to get results in a range of different heights. The slope angle α of a 2D slice with natural roughness was defined by the best-fit line. Runout distances and energy at the first impact point of single-line-segment slopes and 2D slices extracted from four 3D walls were plotted against block release height for combinations of α and σ_r ranges in order to compare the results.

2.2 Calculating the slope roughness and angle of the natural slopes

The roughness of a slope σ_r is defined as the standard deviation of local slope angles within a slope. It is defined as the standard deviation of the slope angle of a segment. An example of roughness calculation for a 2D slice as well as the average, minimum and maximum values corresponding to the associated 20 m segment (from 20 2D slices extracted at every 1 m) is shown in Table 1. Note that the number of 2D slices can be slightly changed from the length of the entire rock wall due to its curvature. Depicted in Table 1 are the α and σ_r values for the maximum height of the slope.

The ledges in natural slopes were removed by replacing them with vertical line segments before calculating α and σ_r by considering the error associated with negative segment angles formed by ledges (Figure 1a-b). Linear regression was applied to compute the best-fit line of a slope to calculate the associated slope angle, α and σ_r was calculated using the weighted slope segment angles (e.g., $\alpha = 69.7^\circ$ and $\sigma_r = 14.8^\circ$ for the maximum height of the 2D slice at $x = 3.5$ m in Table 1). However, in natural 2D slices, the slope segments above the initial location of a rock are not affecting its trajectory or energy. Therefore, α and σ_r of the natural 2D slices were calculated, separately, for each simulation, based on the block release height (Figure 1c). A considerable variation of α and σ_r can be seen even within a 20 m segment. For example, a range of α from 68.2° to 74.4° (mean= 71.7°) and σ_r from 12.1° to 17.3° (mean= 14.1°) can be seen in the 20 m segments shown as an example in Table 1. This demonstrates the

inability of single α and σ_r values to characterize an entire wall or a 20 m segment. Therefore, different slope angles for each 2D slice were used in this study based on the block release height.

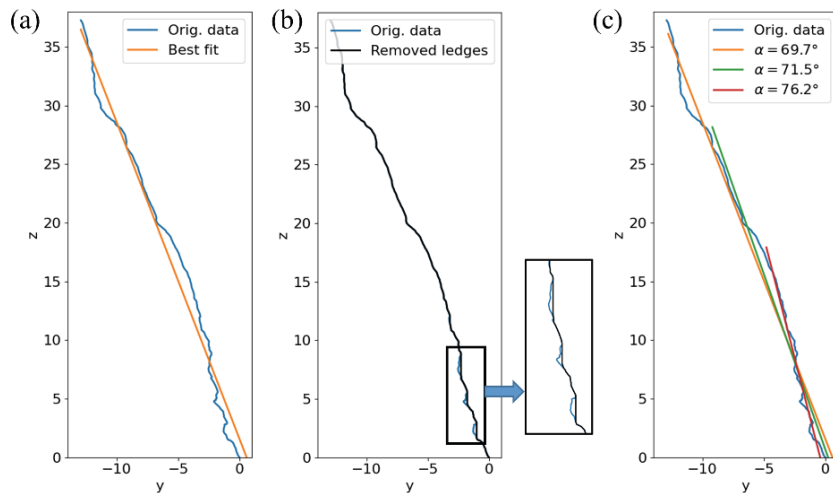


Figure 2. Definition of roughness of a natural slope. (a) The natural slope depicted by a 2D slice (blue line) with its best-fit line for the maximum height (orange line). (b) The Natural slope after removing the ledges (i.e., negative segment angles) with vertical lines (see the magnified section of the slope). (c) The best-fit lines for three block release heights at 37, 27 and 17 m. This will provide the effective slope angle for each block.

Table 1. An example of slope angle and roughness calculation from one of the 20 m segments (C1_005, see Figure 1) based on the maximum height of the slope.

2D slice	α° (best fit)	σ_r° (without ledges)
2D slice at $x = 3.5$ m	69.7	14.8
Average of all 2D slices	71.7	14.1
Min. of all 2D slices	68.2	12.1
Max. of 2D slices	74.4	17.3

2.3 Slope geometry and associated parameters

Single-line-segment slopes are generated with five values of α varying from 60° to 85° with 5° increments and synthetically introduced σ_r , varying from 5° to 25° with 5° increments. For the second approach, four 3D rockfaces with distinct different roughness values were chosen by visual inspection according to their face irregularity as described by Alejano et al. (2008). Table 2 shows the slope characteristics of these four rock walls.

Table 2. The parameters of the four rockfaces selected for this analysis.

Rockwall (triangulated mesh)	Avg. triangle surface (m^2)	Wall height (m)	Wall length (m)	Number of 2D slices	Avg. slope angle ($^\circ$)
F1	0.016	30-48	498	514	69
C1	0.019	39	99	101	70
E1	0.029	39-43	229	220	75
B1	0.010	40	198	180	82

The 3D rockfaces are pre-processed to obtain single long-walls and then rotated to align their strike directions with x-axis. The rock walls are then segmented to 20 m segments to increase the efficiency in data processing, and the segments are re-rotated to fine-align with the x-axis. Then, 2D vertical slices are extracted from these segments. These 2D sections are prepared as RocFall input files and horizontal floors are added to each slope. Thereafter, slope and floor parameters are assigned to these 2D-sections (see Table 3 for the values) based on the results of a sensitivity analysis conducted with different normal and tangential coefficient of restitution, k_n and k_t , and by referring to the coefficient of restitution Table in RocFall User Guide (Rocscience, 2021). The rolling friction angle ϕ is kept constant since it only affects rolling blocks which are seldom in slopes steeper than 45° (Ritchie 1963). The value of ϕ is set to 30° with $\sigma = 2^\circ$ as per the results from in-situ test carried out by Giacomini et al. (2012). These 2D sections represent actual roughness conditions at natural slopes with greater amounts of details. Python scripts are applied to extract the 2D sections, to set all the parameters and to automatically generate RocFall input files (i.e., *.fal8 file format).

Table 3. Parameters assigned to slope and floor materials of the 2D vertical sections extracted from the rockfaces.

	Slope					Floor				
	Distribution	Mean	σ	Min.	Max.	Distribution	Mean	σ	Min.	Max.
k_n	normal	0.6	0.4	0.2	1.0	normal	0.3	0.5	0.2	1.0
k_r	normal	0.6	0.3	0.2	1.0	normal	0.7	0.5	0.2	1.0
φ	normal	30°	2°	24°	36°	normal	30°	2°	24°	36°

2.4 Simulations

Block seeders were set 5 m above the floor with 2 m intervals along the height of the slopes. One hundred blocks were assigned for each block release height to fall under static conditions with a vertical drop height of 0.5 m. The unit mass of 1 kg with a density of 1 kg/m³ is set for all blocks. A lumped mass model is employed for the simulations and k_n is scaled by velocity.

The kinematic rockfall simulations are performed using RocFall which allows exporting of trajectories as ASCII text files. Overall, a total of 1,800,300 trajectories are generated for the 1,015 extracted natural 2D sections, and 69,000 trajectories are generated for the 30 considered single slope profiles with varying α and σ_r combinations. Figure 2a and 2b show the geometries of comparable 2D sections based on natural-slopes and single-line-segments, with rock locations and trajectories.

Finally, the results of both approaches (i.e., single-line-segment based and natural slope based 2D slopes) are compared to evaluate the uncertainty posed by synthetically introduced surface roughness on energies at first impact and runout distances of rockfalls.

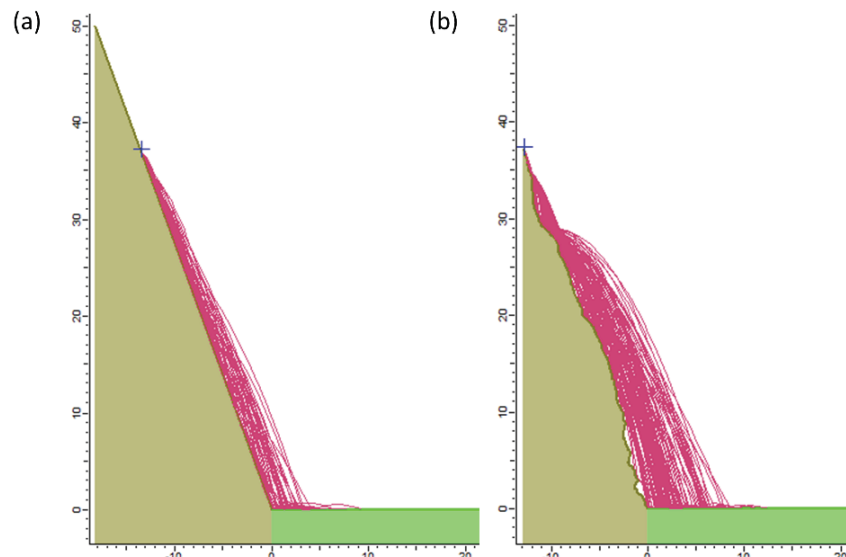


Figure 3. Slope geometries and simulated trajectories of (a) single-line-segment slope, (b) 2D slice extracted from a natural 3D wall. The blue crosses indicate the seeders. One hundred blocks are thrown at each seeder.

3 Results and discussion

The 90th percentile of translational energies (E_{90}) and 95th percentile of runout distances (d_{95}) are considered for the analysis of the results in this work according to the suggestions of rockfall quantitative methodologies and guidelines for rockfall hazard and risk assessment (Mölk et al., 2008; Abbruzzese et al., 2009). The use of maximum values is inadvisable since they are associated with extremely unfavorable conditions, which are unlikely to occur (Pierson et al., 2001). The use of these maximum values for mitigation measures can cause design overestimation leading to significantly high costs. Therefore, E_{90} and d_{95} are, generally, used in protection designs as a reasonable compromise.

To interpret the results, E_{90} and d_{95} are calculated for each seeder for the 100 blocks thrown from the seeder location, i.e., 100 simulations. The results of E_{90} and d_{95} were grouped for each rock wall based on their α - σ_r range combinations (i.e., 20 combinations in total consist of $\alpha = [60^\circ, 65^\circ], [65^\circ, 60^\circ], [70^\circ, 75^\circ], [75^\circ, 80^\circ], [80^\circ, 85^\circ] \times \sigma_r = [5^\circ, 10^\circ], [10^\circ, 15^\circ], [15^\circ, 20^\circ], [20^\circ, 25^\circ]$). The mean and standard deviation of E_{90} and d_{95} for each block release height are then calculated for these groups. Accordingly, 20 plots for these α - σ_r combinations for d_{95} and E_{90} each using large amount of data as explained in Section 2.4 were generated. Results from all four walls, i.e., F1, C1, E1, B1, were plotted with the results of single-line-segment slopes to compare the trends between each 3D wall, and with single-line-segment slopes. However, only four plots were chosen as examples for this paper to depict E_{90} and d_{95} distributions based on the availability of natural 2D slices within these α and σ_r ranges. All the other plots follow

similar trends and are not shown here for brevity. Figs. 3a-b show d_{95} calculated from the RocFall simulation results of 2D slices from natural rock walls and single-line-segment slopes against the block release height (h) for two α - σ_r combinations, i.e., (a) $\alpha=[65^\circ, 70^\circ]$ and $\sigma_r = [10^\circ, 15^\circ]$, (b) $\alpha=[75^\circ, 80^\circ]$ and $\sigma_r = [10^\circ, 15^\circ]$. The E_{90} counterparts of these graphs are shown in Figs. 3c-d.

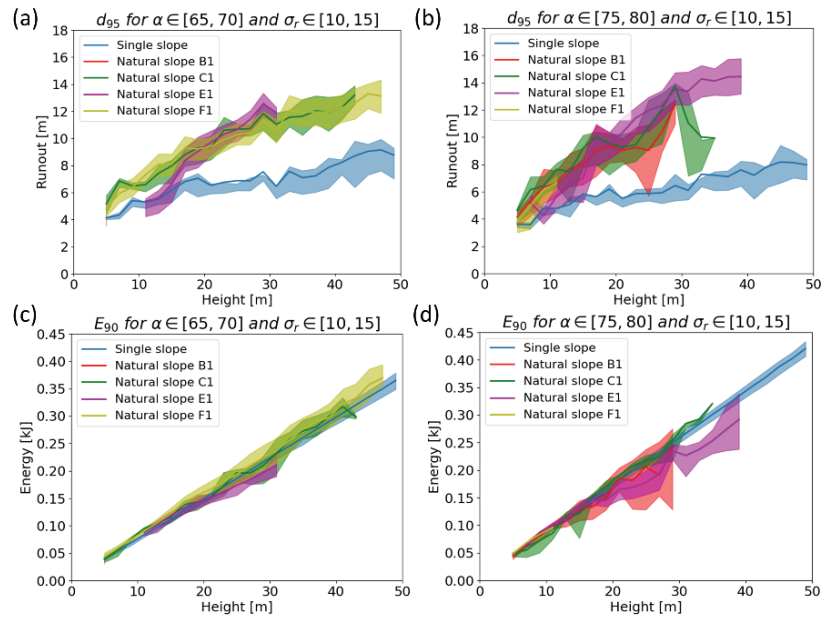


Figure 4. The mean of d_{95} values calculated from the RocFall simulations for the ranges (a) $\alpha=[65^\circ, 70^\circ]$ and $\sigma_r = [10^\circ, 15^\circ]$ (b) $\alpha=[75^\circ, 80^\circ]$ and $\sigma_r = [10^\circ, 15^\circ]$ along with 20 percent and 80 percent quantiles (The lower and upper bounds of the colorized areas show 80 percent and 20 percent quantiles, respectively). Mean with 20 percent and 80 percent quantiles of E_{90} values for the same α - σ_r groups are shown in (c) and (d). Single-line-segment slopes with artificially introduced roughness are shown as single-slopes in these figures.

The d_{95} values calculated in this study are more realistic compared to the simulations performed by Ferrari et al (2016) since the floors were assigned with material parameters. Although the four selected 3D walls showed distinct face irregularities as per visual inspection (Alejano et al., 2008), all of their d_{95} values within a given α - σ_r range followed almost identical trends (see overlapping of natural slopes in Figure 3a-b). In fact, there are instances where the E_{90} values of some of the 3D rockfaces got deviated from their general trend at certain heights (e.g., see rock wall C1 in Figure 3b where E_{90} values deviate from its general trend around $h = 30\text{m}$). These deviations can be possibly associated with the effect from ledges to the results. Although the ledges were removed from the 2D slices, the vertical line segments used to replace ledges can still have an impact on trajectories with respect to the slope angles calculated using best-fit lines, especially for the rocks thrown from higher locations. The entire broad range of d_{95} is not shown by the standard deviation in Figure 3. The effect of outliers within the entire d_{95} range (as shown in Figure 4 as an example) to the result is also noteworthy to mention.

The d_{95} results of single-line-segment slopes show a general underestimation compared to the natural 3D slopes. This can be a result of inability of a single-line-segment to represent the face irregularities of natural slopes which poses uncertainties in d_{95} calculations based on probabilistic rockfall modelling.

However, the E_{90} values of single-line-segment slopes and natural slopes follow closely identical trends (see overlaps in Figure 3c and 3d as examples). However, the natural slopes have a higher range of E_{90} values compared to the single-line-segment slopes. This is also quite obvious when the high irregularities in local slope segment angles and roughness of natural slopes are considered, compared to single-line-segment slopes.

The results clearly depict the uncertainties associated with simulations performed using single-line-segment slopes with respect to the 2D slices extracted from natural slopes since the single-line-segment slopes are unable to capture the irregularities of α and σ_r associated with natural slopes. This explains the necessity of developing models and algorithms based on natural rock slopes by considering their irregularities for more realistic and accurate rockfall simulations for mitigation measures.

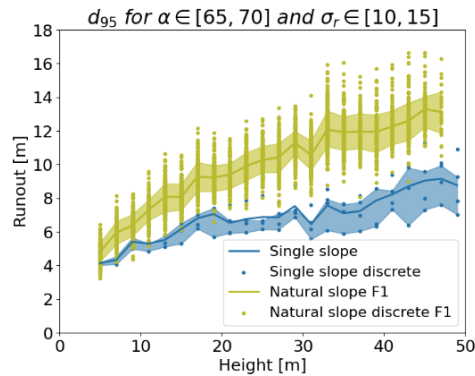


Figure 5. Mean with 20 and 80 percent quantiles (lower and upper bounds of the colored areas, respectively) of d_{95} values calculated for each seeder height for single-line-segment slopes and F1 rockwall of $\alpha=[65^\circ, 70^\circ]$ and $\sigma_r=[10^\circ, 15^\circ]$ with all the data points.

4 Conclusion

This study examines the uncertainties associated with 2D rockfall simulations performed by using single-line-segment rock slopes with artificially introduced roughness by comparing the runout distance and energy at first impact point against 2D slopes extracted from the photogrammetric derived 3D rockface models with natural roughness. The roughness and slope of each 2D slice were calculated separately for each block release height by considering the high variability of α and σ_r values within a rock wall and the effective slope angle for each block. The results show a general underestimation of runout distances calculated by single slope profile rockfall simulations compared to 2D slices extracted with natural roughness. The energy at first impact of single slopes and 3D model based slopes showed a good agreement, yet a higher variability was observed from 3D model based slopes. The results clearly show the importance to include natural slopes and associated irregularities in α and σ_r for rockfall simulations and other predictive analysis tools.

Acknowledgments

This research is funded by the Australian Coal Association Research Program (ACARP, C33040) and the Australian Research Council (DP210101122).

References

- Abbruzzese, J. M., C. Sauthier and V. Labiouse (2009). Considerations on Swiss methodologies for rock fall hazard mapping based on trajectory modelling. *Natural Hazards and Earth System Sciences* 9(4): 1095-1109.
- Alejano, L., H. Stockhausen, E. Alonso, F. Bastante and P. R. Oyanguren (2008). ROFRAQ: A statistics-based empirical method for assessing accident risk from rockfalls in quarries. *International Journal of Rock Mechanics and Mining Sciences* 45(8): 1252-1272.
- Deparis, J., D. Jongmans, S. Garambois, C. Lévy, L. Baillet and O. Meric (2011). Geophysical detection and characterization of discontinuities in rock slopes. *Rockfall Engineering*: 1-37.
- Dorren, L. K. (2003). A review of rockfall mechanics and modelling approaches. *Progress in Physical Geography* 27(1): 69-87.
- Ferrari, F., K. Thoeni, A. Giacomini and C. Lambert (2016). A rapid approach to estimate the rockfall energies and distances at the base of rock cliffs. *Georisk: Assessment and Management of Risk for Engineered Systems and Geohazards* 10(3): 179-199.
- Giacomini, A., K. Thoeni, C. Lambert, S. Booth and S. Sloan (2012). Experimental study on rockfall drapery systems for open pit highwalls. *International Journal of Rock Mechanics and Mining Sciences* 56: 171-181.
- Mölk, M., R. Poisel, J. Weilbold and H. Angerer (2008). Rockfall rating systems: is there a comprehensive method for hazard zoning in populated areas? *Proceedings of the XI Interpraevent 2008 Congress, Dornbirn, Austria* 2: 207-218.
- Pfeiffer, T. J. and T. D. Bowen (1989). Computer simulation of rockfalls. *Bulletin of the association of Engineering Geologists* 26(1): 135-146.
- Ritchie, A. M. (1963). Evaluation of rockfall and its control. *Highway research record* (17).
- Rocscience (2021). RocFall2 UserGuide, <https://www.rocscience.com/help/rockfall/documentation>, Rocscience Inc. [Accessed: 14-June-2022]
- Wyllie, D. C. (2015). Rock fall engineering, CRC Press.